IJBES

International Journal of Built Environment and Sustainability
Published by Penerbit UTM Press, Universiti Teknologi Malaysia
IJBES 11(1)/2024, 33-48

Developing a Performance-Based Approach to the Effect of Roof Features on Fire Safety in Buildings with Atriums

Mehmet Akif Yıldız
Gazi University, Faculty of Architecture, Department of Architecture, Ankara, Turkey.

Figen Beyhan
Gazi University, Faculty of Architecture, Department of Architecture, Ankara, Turkey.

ABSTRACT

Developing technology, changing social structures, and the threat of resource depletion have changed the design of buildings. Therefore, design approaches are developed to increase user comfort and reduce energy consumption by utilizing natural ventilation and lighting. The design of the distribution of outdoor air and light into the spaces through vertical and horizontal gaps reduces the energy demand of the mechanical systems and increases occupant comfort. The atrium is the preferred vertical gap in modern buildings for distributing natural air and light to interior spaces under appropriate conditions. However, in buildings with atrium, there is a risk of fire spreading in the event of a fire due to the uninterrupted gaps between the rooms. It is necessary to ensure the operability of the design by monitoring the measures to be taken in the early stages of design using performance-based fire safety methods. This study develops design strategies for fire analysis in atrium buildings using computational fluid dynamics (CFD) simulation technology. Atrium height, roof type, and slope characteristics are analyzed for the stack effect, which is the main factor in the movement of smoke and flames. As a result of the numerical analyses consisting of flat, unidirectional, and bidirectional sloping roof type, 10, 20, 30-degree roof slope, and one-meter rising atrium roof variables, the effect degrees for smoke dispersal and temperature control are investigated. Fire Dynamic Simulator, which uses CFD capabilities, and Smokeview software, which can visualize the results, were used for the numerical analysis. Correlation analysis was used to determine the effect of variables on temperature. The results showed that flat roofs and designs with increasing height were effective in delaying the spread of smoke and increasing the stack effect in the atrium, while the contribution of roof slope to fire safety was weak.

Article History

Received : *09 June 2023*
Received in revised form : *17 October 2023*
Accepted : *09 November 2023*
Published Online : *31 December 2023*

Keywords:

Atrium, Fire safety, Performance - based approach, Roof features, Computational fluid dynamics

Corresponding Author Contact:

mehmetakif.yildiz@gazi.edu.tr

DOI: 10.11113/ijbes.v11.n1.1175

1. Introduction

Atriums are preferred to provide visually and functionally spacious spaces in buildings, to bring the outdoor environment indoors by bringing uninterrupted natural light from the roof into the atrium, and to increase human interaction. In addition, atriums contribute to the energy efficiency of the building by reducing the need for artificial lighting with natural lighting and providing ventilation and cooling in the interior spaces thanks to the chimney effect. As a result, atriums provide spacious and

comfortable living and working spaces by effectively connecting the outdoor environment with the indoor environment and reducing the burden of lighting, cooling, and ventilating the building with mechanical systems. Despite all the possibilities for efficiency, the fact that the atrium is an uninterrupted space means that in the event of a fire, there is a risk that the fire will spread to the other rooms. Therefore, in buildings where fire safety risks have not been assessed, useful design components will be lost in a potential fire, resulting in loss of life, property safety, and loss of business.

In traditional buildings, horizontal and vertical openings that cause the flow of air indoors are limited to corridors, staircases, lifts, electrical and mechanical shafts (Figure 1). In modern buildings, where user comfort and efficiency are important, openings such as mechanical and electrical shafts, atriums, galleries and double skin facades are added to these openings (Figure 2).

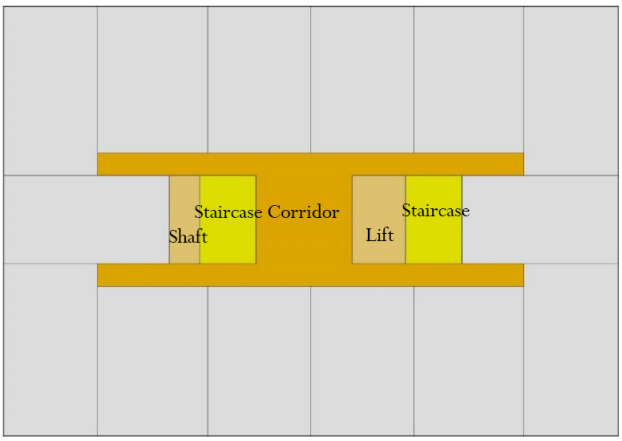

Figure 1 Basic vertical and horizontal openings in traditional buildings

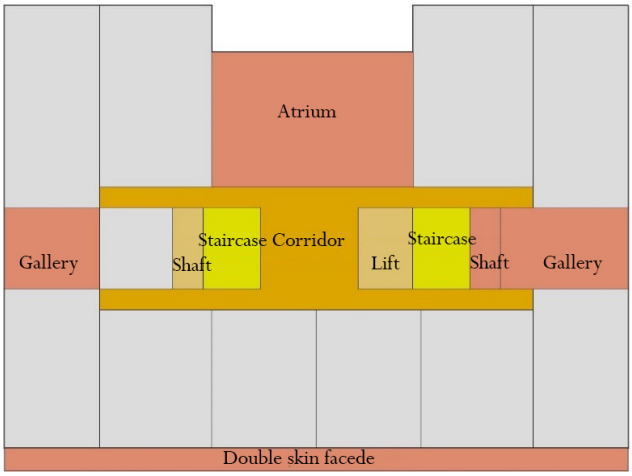

Figure 2 Vertical and horizontal openings in modern buildings

Ventilation in vertical spaces such as the atrium is based on the stack effect system, which is based on the principle of rising heated air. The main force for the stack effect is the difference in temperature and density between indoor and outdoor environments or spaces. When the air temperature interior is higher than outside, the air rises from the lower levels by heating through the gaps with the stack effect and is discharged to the outside through the upper openings of the building. Thus, indoor user comfort is provided by ensuring that the fresh air in the spaces adjacent to the gap is heated and discharged from the space through the gap. It allows the design of natural ventilation using the temperature and pressure difference between the gap and the adjacent spaces and the external environment.

The stack effect is a function of the height of the gap (between the bottom inlet and the top outlet) and the temperature difference between the inside and outside of the opening. In addition to environmental conditions, the stack effect is influenced by factors such as the building's air inlets and outlets, the size of the gap and the characteristics of the spaces associated with the gap. The fact that the gaps designed to improve the efficiency of natural ventilation create uninterrupted vertical and horizontal openings and cause the airflow to move uncontrolled in the interior space is contrary to the traditional methods of fire safety design, which are based on provisions (Doheim, 2012).

Due to the air movement caused by the stack effect in buildings, smoke moves from the high-pressure area to the low-pressure area in vertical spaces. In the case of a fire starting on the lower floors, the pressure inside the building must be higher than the pressure outside to evacuate the smoke from the upper point of the gap. The horizontal plane where there is no pressure difference between the inside and outside of the building is called the neutral plane, where there is no airflow (Mowrer et al., 2004). The neutral plane position is a function of the "absolute temperature ratio". The upward airflow that occurs when the interior is warmer than the external environment is known as the 'normal' stack effect, where warm air flows out of the building through the upper openings. The downward airflow that occurs when the interior is colder than the external environment is known as the "reverse" stack effect, where warm air enters the building through the upper openings and cold air exits the building through the lower openings (Figure 3) (Harrison and Spearpoint, 2006; Mowrer, 2009).

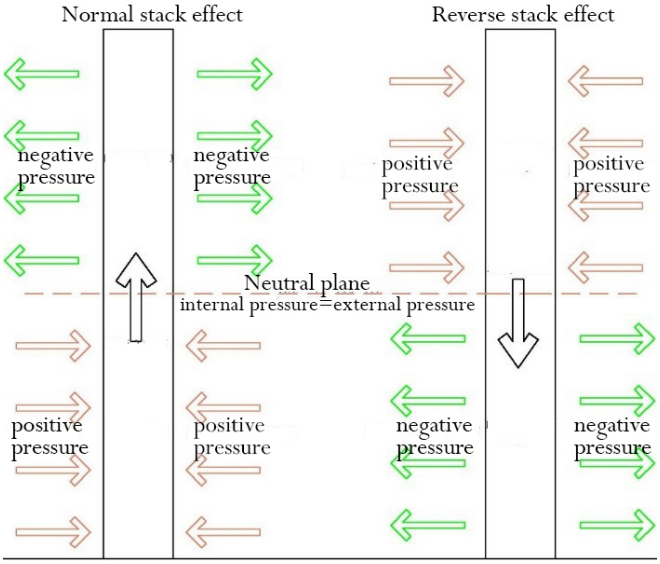

Figure 3 Working principle of the stack effect (Cammelli and Mijorski, 2016)

Natural ventilation strategies based on the rise and fall of heated air in atria create a high-pressure zone in the lower part of the atrium, a low-pressure zone in the upper part, and a neutral plane in between. In this case, as the height of the neutral plane in the atrium increases, the temperature in the upper part of the atrium must be high, as the air heated by the gap is evacuated from the upper part of the atrium without spreading to other rooms (Figure 4) (Cammelli and Mijorski, 2016).

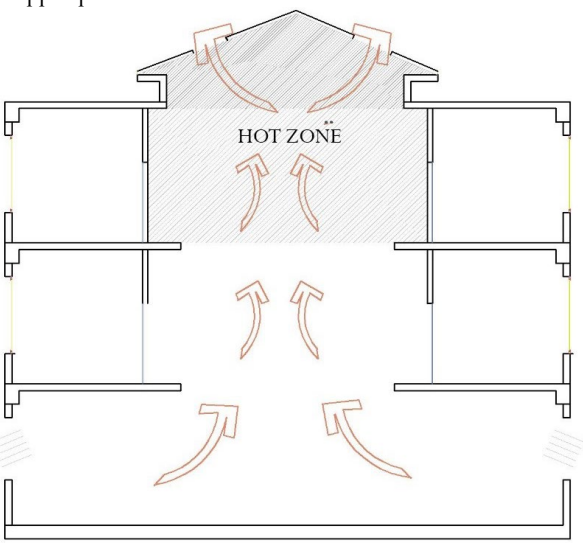

Figure 4 Ventilation in the atrium with the hot zone at the top

Experimental and numerical studies of fire hazards in atria have investigated the characteristics of mechanical smoke exhaust systems, the characteristics of natural ventilation gaps designed in the lower and upper zone of the atrium, the characteristics of ventilation gaps in spaces adjacent to the atrium, and the location and size of the fire. In line with the basic ventilation principle of the atrium, criteria for a high-performance smoke extraction system have been established by analyzing the characteristics of the upper and lower ventilation openings and the design of the smoke extraction systems. Some of these studies have primarily investigated the suitability of mechanical exhaust systems, while others have proposed natural smoke exhaust systems as an alternative to mechanical systems for energy efficiency. Smoke extraction from the atrium ceiling and ventilation openings on the upper floors of the building increased efficiency and reduced the need for mechanical extraction systems (Zhang et al., 2021; Fang et al., 2022; Al-Waked et al., 2021; Chow and Li, 2010). Some studies have compared full-scale experiment and computational fluid dynamics analysis with scenarios consisting of natural and mechanical exhaust systems and fire origin location and size to analyse smoke layer, pressure and temperature levels in the atrium. Since the smoke, temperature, and pressure levels of the full-scale experimental results and the computer simulation results were similar, it has been demonstrated that results can be obtained more quickly and economically for atrium fire design without full-scale testing. (Cantizano et al., 2023; Montes et al., 2009; Montes et al., 2008; Barsim et al., 2020).

In the scenarios consisting of the variables of fire starting in the center of the atrium or the spaces adjacent to the atrium, changing the characteristics of the mechanical smoke exhaust systems, it was found that the spread area and speed of the fire starting in the center of the atrium were high. In addition, mechanical exhaust systems and the design of smoke barriers in appropriate locations have been effective in limiting and reducing the spread of smoke (Jiao et al., 2023; Brzezinska and Brzezinska, 2022). Numerical analyses of scenarios consisting of the rate and position of ventilation openings in the atrium and the spaces adjacent to the atrium have shown that the location of ventilation openings in the roof and upper parts of the atrium is efficient for smoke removal and temperature rise at the upper points. Increasing the size of the natural smoke evacuation openings has effectively improved smoke evacuation (Wang et al., 2021; Qin et al., 2009). In recent studies, horizontal and vertical obstacles have been designed to control smoke by interfering with conventional natural ventilation systems in high-rise atriums with inlet openings at the bottom and outlet openings at the top. In these studies, a segmentation panel was used to divide the atrium horizontally into upper and lower sections to limit the movement of smoke (Sha et al., 2022; Sha et al., 2023). In addition, smoke curtains were designed to separate the atrium area vertically. In atrium designs with similar ventilation configurations, the smoke curtain and panel layout have been effective design tools in managing smoke diffusion and the pressure differential between the atrium and the outside (Gomez et al., 2020; Yuen et al., 2019).

This study investigated the effects of atrium height, atrium roof type, and slope on smoke removal and temperature levels to contribute to studies of mechanical and natural smoke removal systems, ventilation opening size, and position. It was found that designing the atrium height above the building height and increasing the volume of the atrium at the upper level contributed to smoke evacuation and temperature control.

2. Methodology

Computational fluid dynamics (CFD) computer simulation for fire analysis and smoke control systems has been widely used in recent years. CFD technology solves complex equations and analyses the movement and time behavior of fluids in three-dimensional systems. The atrium is the subject of CFD analysis as it is critical for human safety in a fire. The Fire Dynamics Simulator (FDS), which includes CFD features, is used in this study to control smoke layer height and temperature.

This study, based on stack effect ventilation strategies in the atrium, examines smoke spread and temperature levels as a function of pressure change in the event of a fire starting in the atrium space. Unlike the physical modeling studies in the literature, the effect of atrium roof type, slope, and height on fire is investigated. The effects of the most popular flat, unidirectional, and bidirectional roof types and the height of the rooftop on smoke propagation and temperature are analyzed. The study only analyses roof type, slope, and height and ignores other design components that affect fire spread.

Correlation analysis was performed with the simulation results obtained to determine the degree of contribution of the roof design features to the stack effect in the atrium and the temperature levels in the rooms. Correlation analysis, which is a statistical analysis method, calculates the measure of change between variables. For the correlation coefficient, which mathematically takes a value between -1 and +1, a value close to 0 indicates a weak effect, close to 1 indicates a strong positive effect, and close to -1 indicates a strong negative effect. In addition, a negative correlation coefficient indicates that one of the variables is increasing while the other is decreasing, and a positive correlation coefficient indicates that one of the variables is increasing while the other is increasing.

2.1. Prototype Building Design

The 3-storey prototype building, with an atrium space of 400 x 600 x 1050 cm (width x length x height) in the center and 400 x 400 x 350 cm rooms on each floor around the atrium space, was designed without taking into account the effect of climatic elements such as location and prevailing wind. Two air outlets are placed on the atrium ceiling (Figure 5).

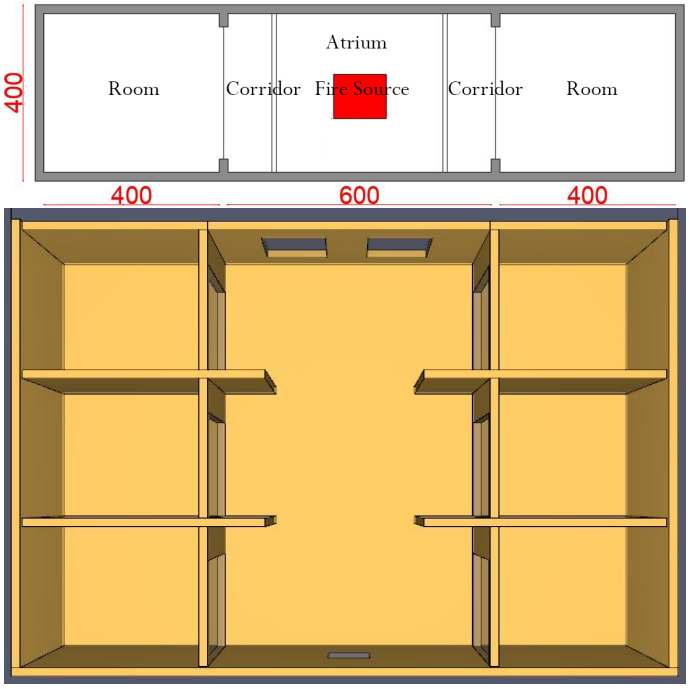

Figure 5 Prototype building plan and section

In order to examine the effect of roof type, slope, and height on fire in the prototype building, three types of design scenarios were determined flat roof, one-way and two-way sloping. For the flat roof, four scenarios were designed starting from the building height level and rising at 1-meter intervals. For unidirectional and bidirectional sloping roofs, the roof slope is determined as 10, 20, and 30 percent and the design scenarios are given in Table 1.

Table 1 Numerical model design scenarios

Scenario	Roof type	Height (cm)	Slope (%)
A1	Flat	1050	0
A2	Flat	1150	0
A3	Flat	1250	0
A4	Flat	1350	0
B1	Unidirectional	1100	10
B2	Unidirectional	1170	20
B3	Unidirectional	1240	30
C1	Bidirectional	1100	10
C2	Bidirectional	1135	20
C3	Bidirectional	1175	30

2.2. Design Fire and Numerical Model Features

Studies presenting performance-based approaches use the t-squared fire, where the rate of combustion varies in proportion to the square of time. The curve expressing the ratio of burn rate to the square of time for a t-squared fire shows the time required to reach the highest heat release rate. The heat release rate gives the most important information about how much heat is released when combustible materials burn. If the heat release rate is known, the smoke temperature, smoke layer thickness, smoke flow rate, radiant heat flux and the result of the effect on combustible materials and structural elements in the enclosed volume are known. T² fire, that is the rate of heat release, is given by equation 1:

$$Q=\alpha t^{p} \quad \text{(Eq. 1)}$$

Q:Heat release rate Btu/s (kW)
α:Fire growth coefficient Btu/s3 (kW/s^2),
t: Time from ignition (s)
p:Positive exponent

According to the NFPA 92 Standard of Smoke Control Systems, the fire growth rate is classified as slow, medium, fast, and

ultra-fast and the reference heat release rate is 1055 kW. The fire growth curve for slow, medium, fast and ultra-fast growth rates to achieve the reference heat release rate of 1055 kW is shown in Figure 6 (NFPA, 2021). In the study, the reference heat release rate is calculated as 1055 kW and the fire growth rate is calculated as fast.

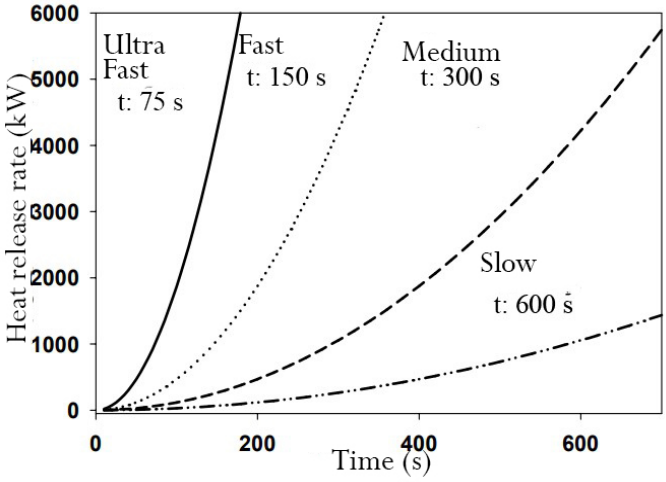

Figure 6 Fire growth curve and time for the fire to reach the reference heat release rate (Bwalya et al., 2004)

The time to reach the reference heat release rate for the fast fire growth curve is 150 seconds, and the fire growth coefficient (α) is calculated to be 0.047 kW/s^2 from Equation 1. The 100 x 100 cm reaction source on the atrium floor was selected as the polyurethane GM27, consisting of 1.00 carbon, 1.7 hydrogen, 0.3 oxygen, and 0.08 nitrogen atoms. For this reaction source, smoke production is 0.198 g/g and carbon monoxide (CO) production is 0.042 g/g. Table 2 shows the characteristics of the design fire (Hurley, 2016).

Table 2 Design fire features

Feature	Value
Fire type	Flaming fire
Reaction type	Polyurethane GM27
Fire growth	t2 fire
Smoke production	0,198 g/g
CO production	0,042 g/g
Heat release rate	1055
Fire growth coefficient	0,047
Simulation time	150 s

FDS software, which can present computational fluid dynamics together with simulation, and Smokeview software, which can visualize the results, were used for numerical analysis. CFD generates solutions for the conservation of mass, momentum, pressure, and turbulence using the Navier-Stokes equations (Mc Grattan et al., 2013). The study used the Pyrosim program, which includes FDS functions and Smokeview visualization, to define boundaries and create geometry. To generate the three-dimensional model in Pyrosim, the lengths of the mesh cell structure where the boundary conditions were determined were set to 0.2x 0.2 x 0.2 m. Three thermocouples were placed at the atrium floor level, ceiling level, and in one of the last floor rooms to measure the temperature, and slices were placed in x2 direction to monitor the temperature and smoke movement (Figure 7).

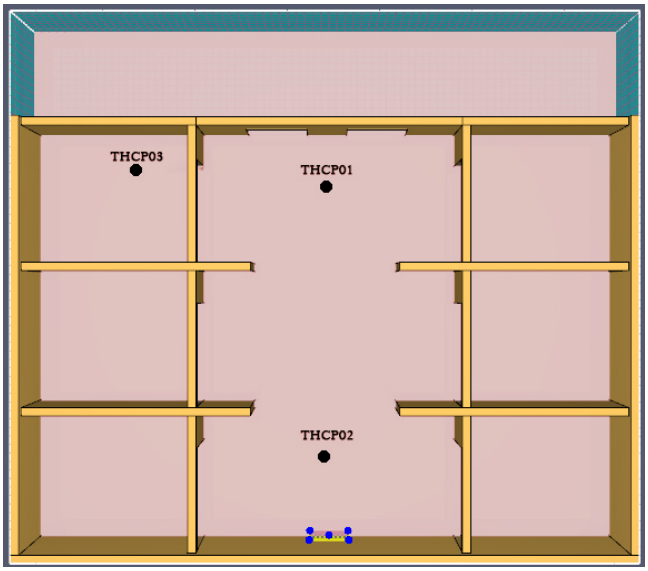

Figure 7 The numerical model obtained from Pyrosim

3. Findings

In the A1 scenario, the smoke reached the atrium ceiling at the 23rd second and exited through the air outlet. At the 45th second, smoke began to spread to the last floor rooms, at the 64th second to the first floor rooms, and at the 90th second to the rooms on the ground floor. At 105th second, the last floor and 115th second, the first floor rooms were completely smoke-filled (Figure 8). While the highest ambient temperature of 300.17 ^{0}C was reached at 148th second, the highest temperature was 86.81 ^{0}C at the ceiling of the atrium and the highest temperature was 37.55 ^{0}C in the last floor room (Figure 9).

Figure 8 A1 scenario smoke view

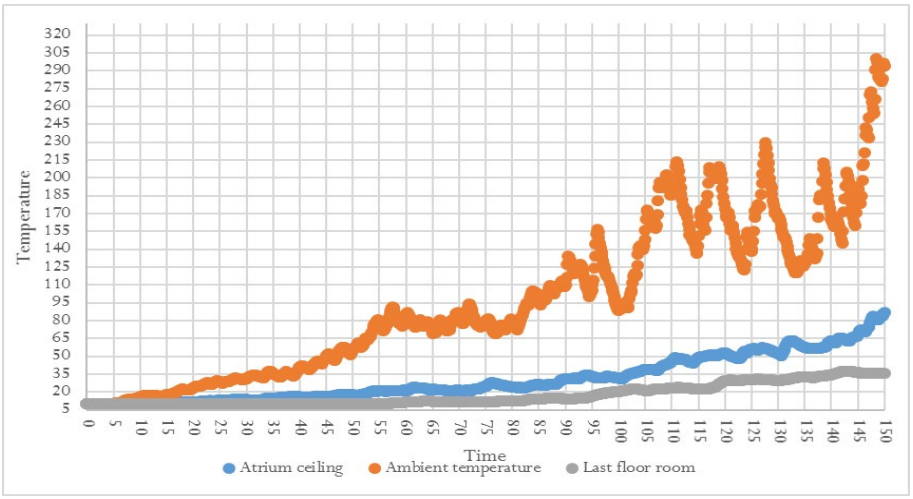

Figure 9 A1 scenario time-dependent temperature values

In the A2 scenario, the smoke reached the atrium ceiling at the 28th second and exited through the air outlet. At the 54th second, smoke began to spread to the last floor rooms, at the 64th second to the first floor rooms, and at the 90th second to the rooms on the ground floor. At 105th second, the last floor and 115th second, the first floor rooms were completely smoke-filled (Figure 10). While the highest ambient temperature of 308.95 ^{0}C was reached at 138th second, the highest temperature was 70.55 ^{0}C at the ceiling of the atrium and the highest temperature was 35.27 ^{0}C in the last floor room (Figure 11).

Figure 10 A2 scenario smoke view

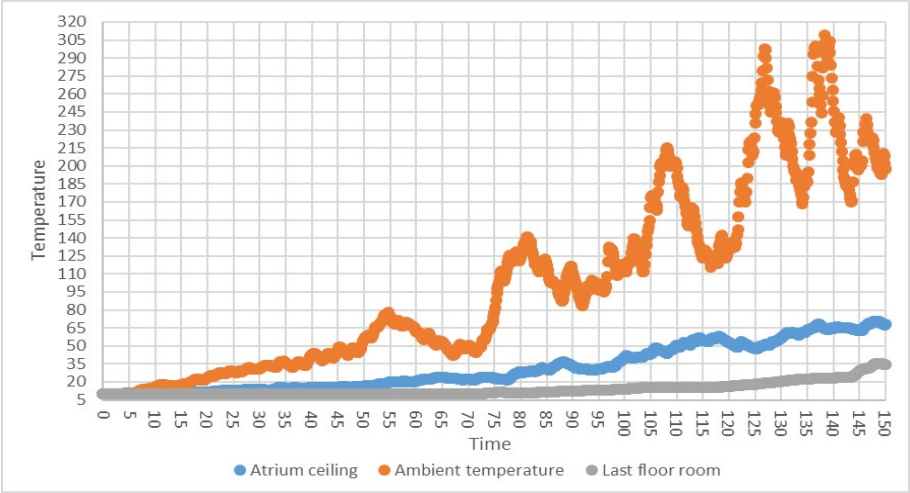

Figure 11 A2 scenario time-dependent temperature values

In the A3 scenario, the smoke reached the atrium ceiling at the 30th second and exited through the air outlet. At the 60th second, smoke began to spread to the last floor rooms, at the 67th second to the first floor rooms, and at the 96th second to the rooms on the ground floor. By the 115th second, the last floor and the rooms on the first floor were filled with smoke (Figure 12). While the highest ambient temperature of 307.42 ^{0}C was reached at 133th second, the highest temperature was 82.83 ^{0}C at the ceiling of the atrium and the highest temperature was 33.09 ^{0}C in the last floor room (Figure 13).

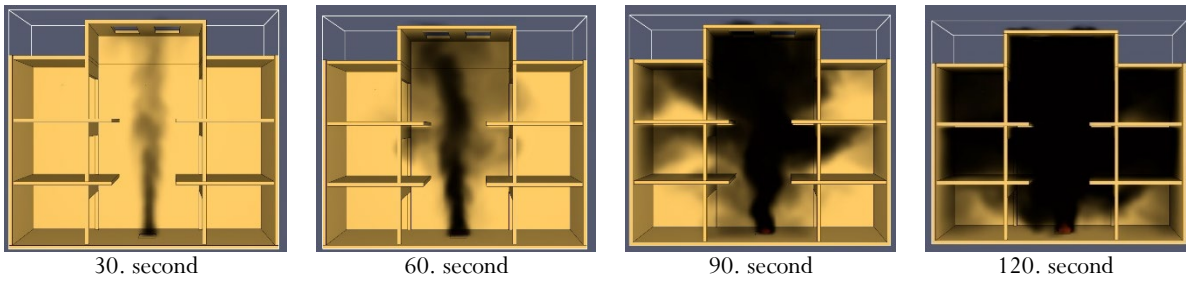

Figure 12 A3 scenario smoke view

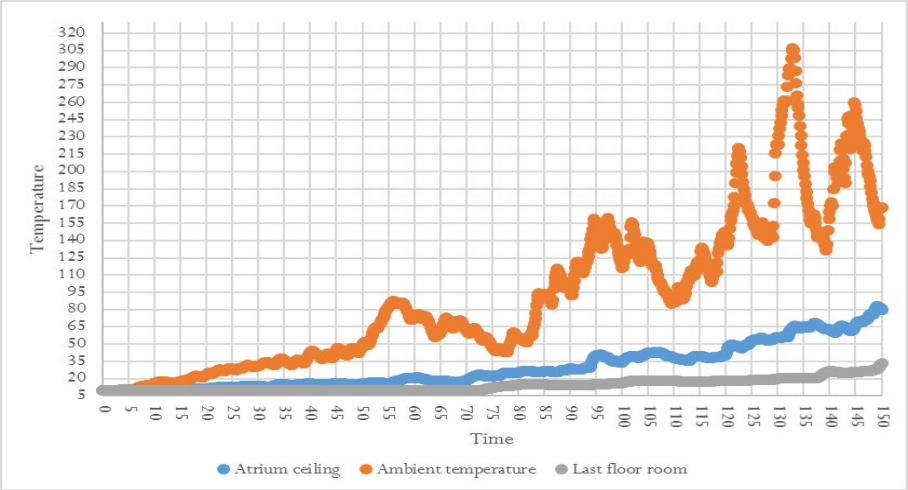

Figure 13 A3 scenario time-dependent temperature values

In the A4 scenario, the smoke reached the atrium ceiling at the 31th second and exited through the air outlet. At the 66th second, smoke began to spread to the last floor rooms, at the 69th second to the first floor rooms, and at the 100th second to the rooms on the ground floor. By the 125th second, the last floor and the rooms on the first floor were filled with smoke (Figure 14). While the highest ambient temperature of 300.64 ^{0}C was reached at 146th second, the highest temperature was 84.24 ^{0}C at the ceiling of the atrium and the highest temperature was 21.96 ^{0}C in the last floor room (Figure 15).

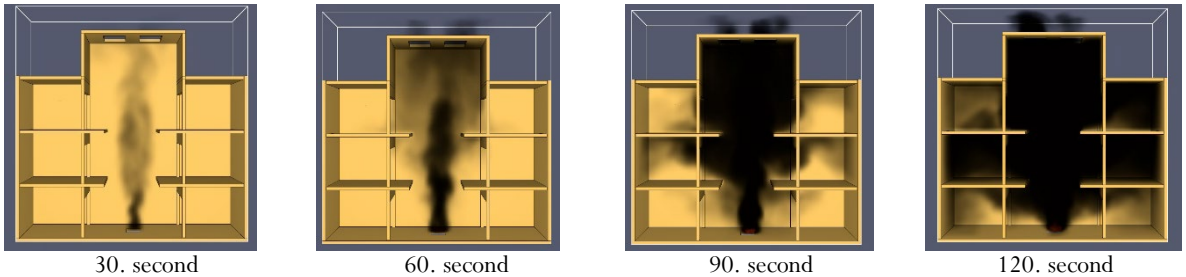

Figure 14 A4 scenario smoke view

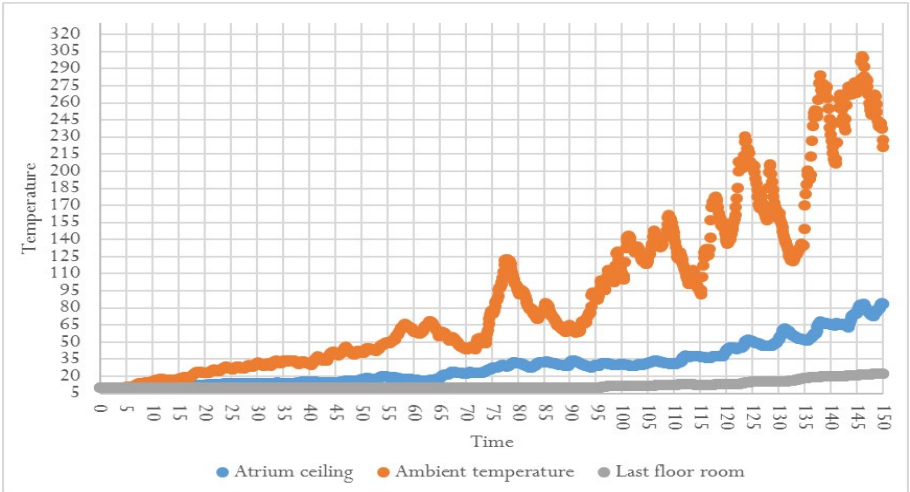

Figure 15 A4 scenario time-dependent temperature values

In the B1 scenario, the smoke reached the atrium ceiling at the 24th second and exited through the air outlet. At the 50th second, smoke began to spread to the last floor rooms, at the 65th second to the first floor rooms, and at the 82nd second to the rooms on the ground floor. At 105th second, the last floor and 120th second, the first floor rooms were completely smoke-filled (Figure 16). While the highest ambient temperature of 276.64 ^{0}C was reached at 149th second, the highest temperature was 67.46 ^{0}C at the ceiling of the atrium and the highest temperature was 42.30 ^{0}C in the last floor room (Figure 17).

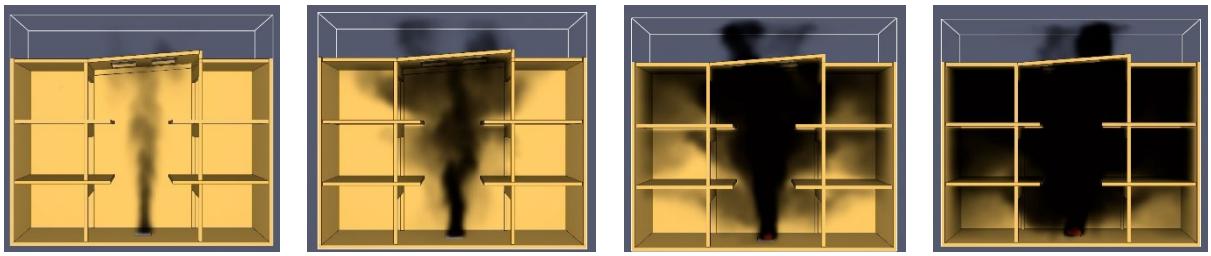

Figure 16 B1 scenario smoke view

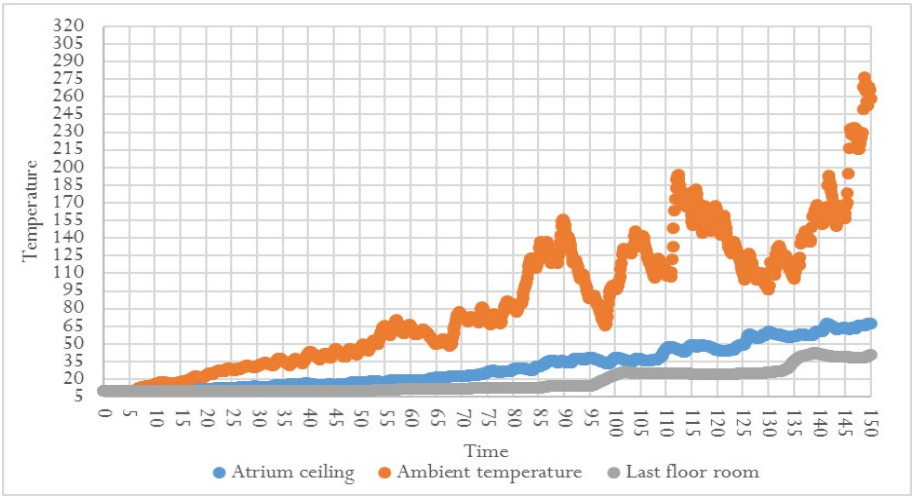

Figure 17 B1 scenario time-dependent temperature values

In the B2 scenario, the smoke reached the atrium ceiling at the 24th second and exited through the air outlet. At the 50th second, smoke began to spread to the last floor rooms, at the 60th second to the first floor rooms, and at the 90th second to the rooms on the ground floor. At 100th second, the last floor and 115th second, the first floor rooms were completely smoke-filled. The tendency of the smoke to spread into the rooms was mainly towards the rooms on the side where the roof slope was high (Figure 18). While the highest ambient temperature of 192.39 ^{0}C was reached at 104th second, the highest temperature was 76.74 ^{0}C at the ceiling of the atrium and the highest temperature was 36.46 ^{0}C in the last floor room (Figure 19).

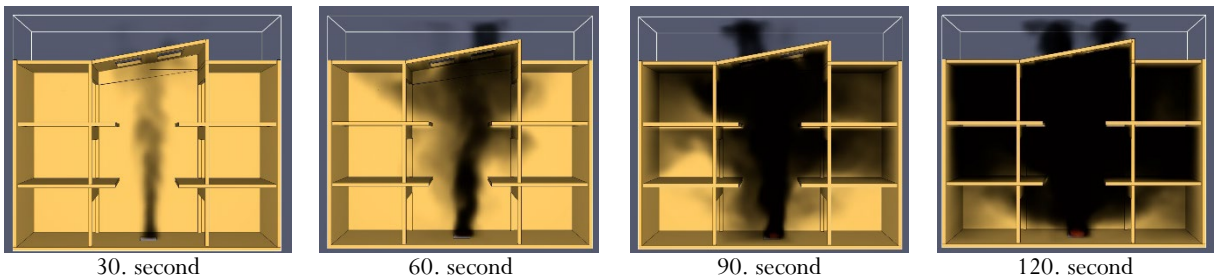

Figure 18 B2 scenario smoke view

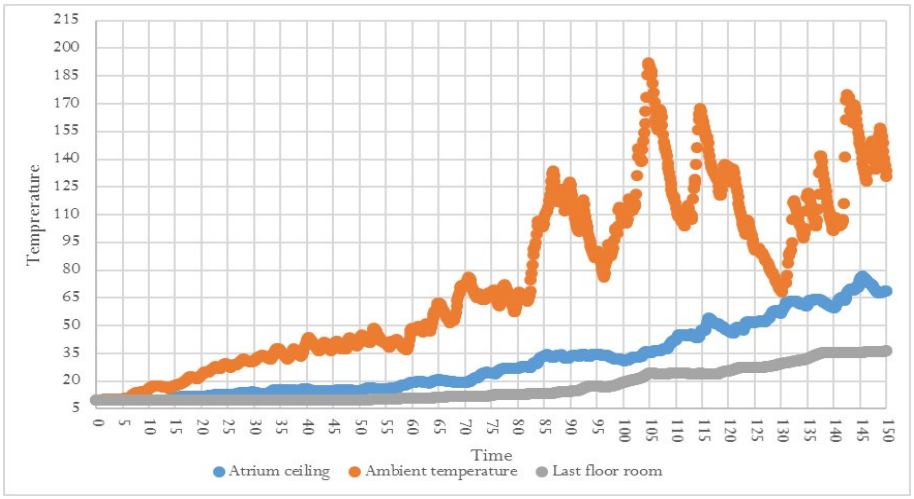

Figure 19 B2 scenario time-dependent temperature values

In the B3 scenario, the smoke reached the atrium ceiling at the 24th second and exited through the air outlet. At the 52nd second, smoke began to spread to the last floor rooms, at the 62th second to the first floor rooms, and at the 95th second to the rooms on the ground floor. At 105th second, the last floor and 120th second, the first floor rooms were completely smoke-filled. The tendency of the smoke to spread into the rooms was mainly towards the rooms on the side where the roof slope was high (Figure 20). While the highest ambient temperature of 300.82 ^{0}C was reached at 137th second, the highest temperature was 74.35 ^{0}C at the ceiling of the atrium and the highest temperature was 27.96 ^{0}C in the last floor room (Figure 21).

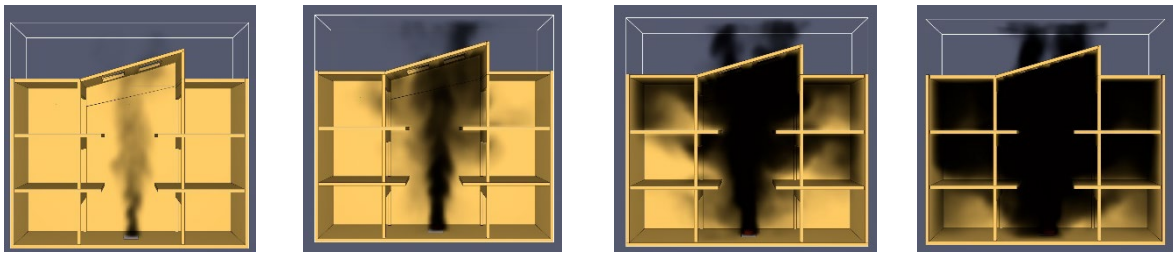

30. second 60. second 90. second 120. second

Figure 20 B3 scenario smoke view

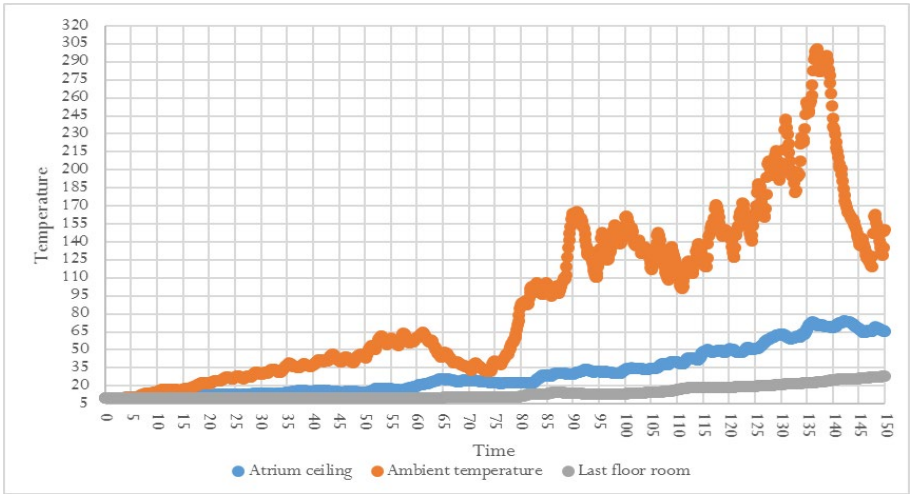

Figure 21 B3 scenario time-dependent temperature values

In the C1 scenario, the smoke reached the atrium ceiling at the 24th second and exited through the air outlet. At the 52nd second, smoke began to spread to the last floor rooms, at the 67th second to the first floor rooms, and at the 88th second to the rooms on the ground floor. At 100th second, the last floor and 115th second, the first floor rooms were completely smoke-filled (Figure 22). While the highest ambient temperature of 267.54 ^{0}C was reached at 138th second, the highest temperature was 75.02 ^{0}C at the ceiling of the atrium and the highest temperature was 46.19 ^{0}C in the last floor room (Figure 23).

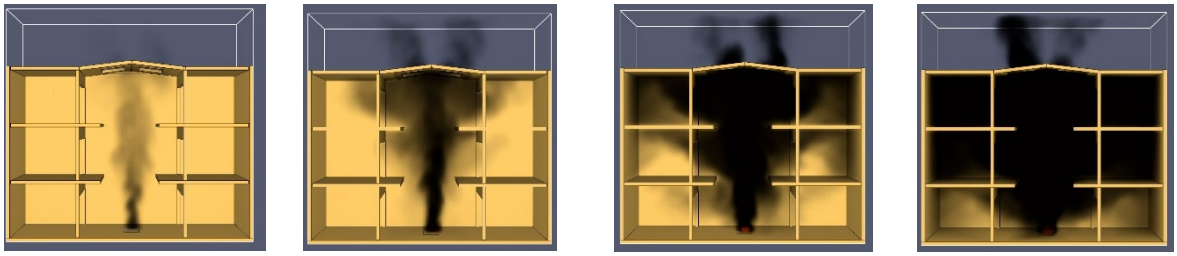

Figure 22 C1 scenario smoke view

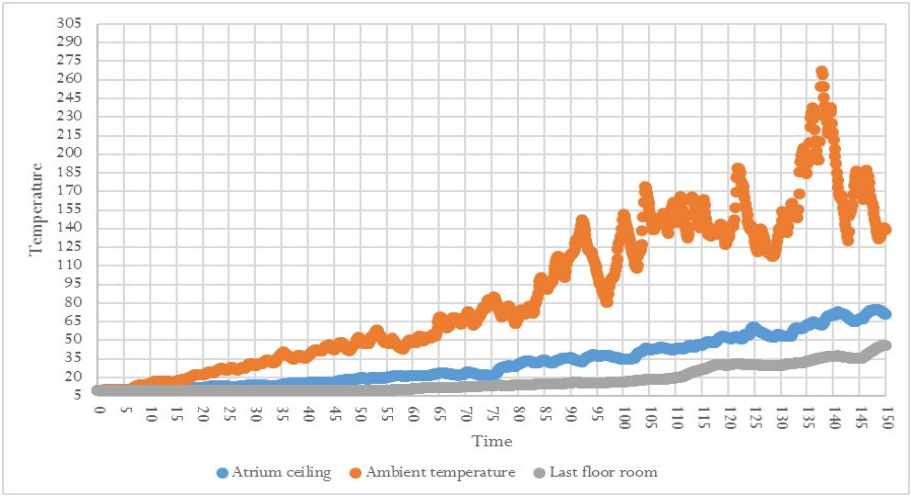

Figure 23 C1 scenario time-dependent temperature values

In the C2 scenario, the smoke reached the atrium ceiling at the 23rd second and exited through the air outlet. At the 48th second, smoke began to spread to the last floor rooms, at the 65th second to the first floor rooms, and at the 85th second to the rooms on the ground floor. At 100th second, the last floor and 115th second, the first floor rooms were completely smoke filled (Figure 24). While the highest ambient temperature of 249.65 ^{0}C was reached at 145th second, the highest temperature was 79.33 ^{0}C at the ceiling of the atrium and the highest temperature was 42.76 ^{0}C in the last floor room (Figure 25).

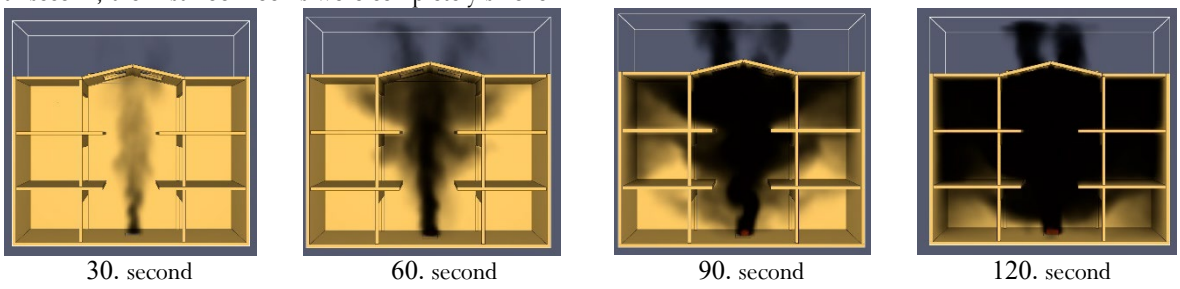

Figure 24 C2 scenario smoke view

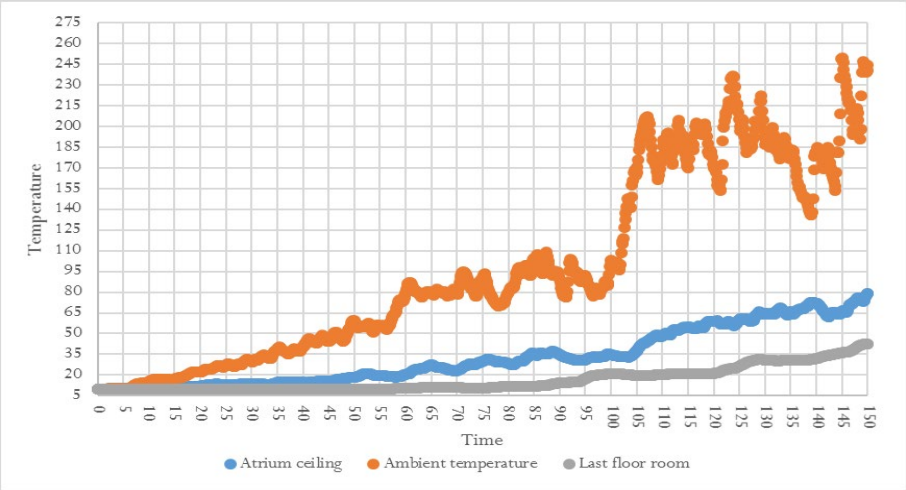

Figure 25 C2 scenario time-dependent temperature value

In the C3 scenario, the smoke reached the atrium ceiling at the 24th second and exited through the air outlet. At the 47th second, smoke began to spread to the last floor rooms, at the 62nd second to the first floor rooms, and at the 88th second to the rooms on the ground floor. At 105th second, the last floor and 115th second, the first floor rooms were completely smoke-filled (Figure 26). While the highest ambient temperature of 266.51 ^{0}C was reached at 148th second, the highest temperature was 76.35 ^{0}C at the ceiling of the atrium and the highest temperature was 34.10 ^{0}C in the last floor room (Figure 27).

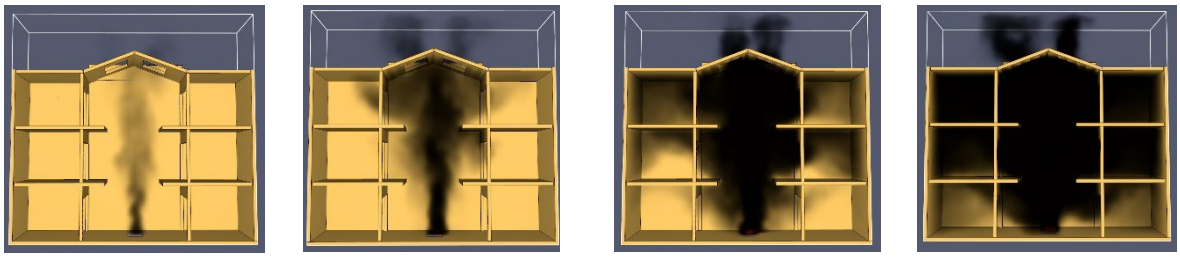

Figure 26 C3 scenario smoke view

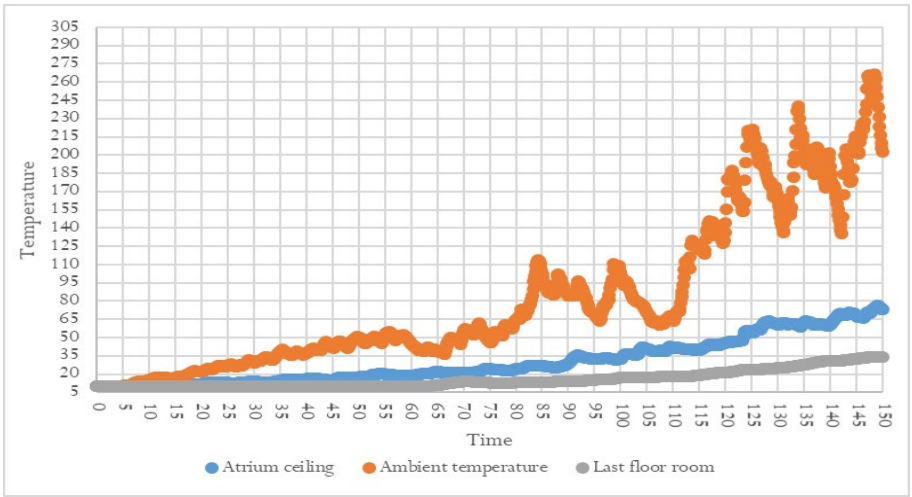

Figure 27 C3 scenario time-dependent temperature value

4. Evaluation and Conclusion

In a fire event, smoke rises rapidly vertically until it encounters a horizontal obstacle. When the smoke reaches the horizontal obstacle, it slowly spreads along the horizontal surface and moves downwards again. In the scenarios in this study where this theoretical knowledge is analyzed in practice, the smoke rises rapidly until it reaches the atrium ceiling and then moves along the ceiling surface and downwards. As a result of increasing the height of the flat roof in the A scenarios, the duration of the smoke on the roof surface increased, and the process of smoke penetration into the rooms was delayed. In the A1 scenario where the roof surface is at the level of the building height, the first spread of smoke into the room started at 45 seconds, while in the A4 scenario where the roof surface is designed to be 300 cm above the building height, the smoke spread into the room started at 66 seconds. This situation shows that taking into account the fast fire growth rate in the numerical analysis, designing the atrium roof flat and increasing its height contribute positively to the escape time of people.

In Scenarios B and C, where the roof is designed as a unidirectional and bidirectional sloping roof, the change in volume area at the building height is small between the scenarios, so the downward movement time of the smoke from the ceiling surface is not different. In the B scenarios, where the roof sloped in one direction, as the smoke spread towards the area where the slope increased, the smoke spread from the ceiling into the rooms was also in the direction where the slope was higher.

As the stack effect in the cavity increases with temperature due to the increase in pressure, the higher temperature level at the upper level of the atrium compared to the lower regions raises the position of the neutral plane in the gap and assists the evacuation of smoke from the atrium roof. Since the ambient temperature level is variable in the scenarios, the rate of the temperature at the upper level of the atrium to the temperature at the floor level of the atrium was calculated and compared.

Measures of central tendency were used to statistically describe the temperature values. Measures of central tendency are critical points that provide an interpretation of the distribution and are expressed by the mean or median for numerical data. If the numerical data show a normal distribution, the mean is used, and if the numerical data show an irregular distribution, the median is used. Looking at the graphs of the temperature values in the Results title, we can see that the temperature has an increasing graphic, so the mean was calculated for the analysis. The mean temperatures of the atrium floor, the atrium ceiling and one of the rooms on the last floor in the scenarios are shown in Table 3.

Table 3 Mean temperature values of the scenarios

Scenario	Roof type	Height (cm)	Slope (%)	Atrium floor	Atrium ceiling	Last floor room	Atrium temperature rate*
A1	Flat	1050	0	151.99	48.4	22.73	0.32
A2	Flat	1150	0	103.63	39.9	22.14	0.39
A3	Flat	1250	0	89.36	45	21.54	0.50
A4	Flat	1350	0	115.71	46.77	15.98	0.40
B1	Unidirectional	1100	10	134.45	38.45	25.43	0.29
B2	Unidirectional	1170	20	70.27	39.29	23.23	0.56
B3	Unidirectional	1240	30	80.1	37.62	18.98	0.47
C1	Bidirectional	1100	10	74.58	40.58	28	0.54
C2	Bidirectional	1135	20	127.15	44.66	26.38	0.35
C3	Bidirectional	1175	30	106.47	41.44	22.05	0.39
* Rate of atrium ceiling temperature to atrium floor temperature							

Considering the temperature rate in the atrium, it can be seen that the stack effect is efficient for A3 of the flat roof type scenarios, B2 of the unidirectional sloping roof type scenarios and C1 of the bidirectional sloping roof type scenarios. Scenario A4, with the lowest room temperature, has the most appropriate design for the user limit.

Due to the numerical analysis of the scenarios determined by CFD with the variables consisting of the roof design characteristics, a statistical analysis was used for the degree of change of the temperature values of the scenarios with the increase of height, slope, and roof type. In this case, correlation analysis was performed for the dependent variables of atrium temperature rate and last floor room temperature to determine the degree of influence of the variables. The correlation of the atrium temperature raw, which gives an idea of the strength of the stack effect in the atrium, between the variables is shown in Table 4. According to the table, roof type has an effect of 0.12, height has a positive effect of 0.30, slope has a positive effect of

0.17 on the dependent variable, and since the correlation value is far from 1, there is a positive weak correlation.

Table 4 Correlation of variables with atrium temperature rate

	Atrium temperature rate	Roof type	Height	Slope
Atrium temperature rate	1			
Roof type	0.124934366	1		
Height	0.299287613	-0.31478	1	
Slope	0.174066669	0.743256	-0.009256556	1

The correlation between the temperature value of the room on the last floor with the highest temperature increase among the rooms on all floors and the variables is shown in Table 5. According to the table, roof type has a positive effect of 0.60, height has a positive effect of 0.81, and slope has a positive effect of 0.10 on the dependent variable. There is a strong negative correlation between height and temperature, and the temperature decreased as the height increased. As the roof type is a qualitative variable, it was not interpreted as a positive or negative correlation, but the lowest temperature values were observed for the flat roofs and the highest for the bidirectional roofs.

Table 5 Correlation of variables with last floor room

	Last floor room	Roof type	Height	Slope
Last floor room	1			
Roof type	0.604520209	1		
Height	-0.811536301	-0.31478	1	
Slope	0.102912665	0.743256	-0.009256556	1

In this study, in which the numerical analysis of the fire safety design was carried out using a performance-based modeling approach, only the characteristics of the atrium roof were considered as design variables, neglecting climatic data and other active and passive design features. The design of the atrium ceiling above the building height increased the atrium chimney effect and contributed positively to the extraction of smoke through the air outlet on the atrium ceiling. In flat roof scenarios with atrium heights of 2 and 3 meters above building height, the

time for smoke to reach the atrium ceiling was reduced, and the time to remain smoke on the ceiling for occupant evacuation was increased compared to unidirectional and bidirectional pitched roofs. In scenarios with sloping roof designs, smoke density and residence time of smoke at the atrium ceiling level were shortened, and the orientation of smoke to the spaces was increased compared to flat roofs. The studies in the literature where the physical properties of the atrium are the subject of fire safety design have examined the height and width of the atrium, its location, its relationship with the spaces in the building, and the atrium form by numerical analysis. As a contribution to the studies in the literature, this study examined the physical properties of the atrium roof with air outlets for natural ventilation and natural smoke exhaust system. It examined the relationship between the most suitable roof shape and height and the chimney effect caused by internal and external temperature and pressure differences. Thus, atrium roof design criteria for smoke extraction and temperature control through the atrium roof were presented for both academic studies and the building industry.

Acknowledgements

The authors express their gratitude to the reviewers whose valuable input significantly enhanced the quality of this manuscript.

References

Al-Waked, R., Nasif, M., Groenhout, N., & Partridge, L. (2021). Natural ventilation of residential building Atrium under fire scenario. *Case Studies in Thermal Engineering*, 26: 101041- 101051.

Barsim, M., Bassily M. A., El-Batsh, M. H., Rihan, Y. A., & Sherif M. M. (2020). Numerical simulation of an experimental atrium fires in combined natural and forced ventilation by CFD. *International Journal of Ventilation*. 19(1): 201-223.

Brzezinska, M., & Brzezinska, D. (2022). Contemporary atrium architecture: a sustainable approach to the determination of smoke ventilation criteria in the event of a fire. *Energies,* 15(7): 2484.

Bwalya, A. C., Sultan, M. A., & Benichou, N. (2004). *Design fires for fire safety engineering: a state-of-the-art review*. Paper presented at CIB World Building Congress, Rotterdam, Netherlands, 2-7 May.

Cantizano, A., Ayala, P., Arenas, E., Perez, J. R., & Montes, C., G. (2023). Numerical and experimental investigation on the effect of heat release rate in the evolution of fire whirls. *Journal of Fire Protection Engineering Case Studies in Thermal Engineering*, 41: 102513-102525.

Chow, C. L., & Li, J. (2010). An analytical model on static smoke

exhaust in atria. *Journal of Civil Engineering and Management,* 16(3): 372–381.

Doheim, R. (2011). Towards an architectural strategy for early integration of natural smoke ventilation in retail buildings. Doctor of Philosophy, The University of Ulster, Ulster, 31-41.

Fang, X., Yuen, A. C. Y., Yeoh, H. G., Lee, E. W. M., & Cheung, S. C. P. (2022) Numerical study on using vortex flow to improve smoke exhaust efficiency in large-scale atrium fires. *Indoor and Built Environment,* 32(1): 98-115.

Gomez, R. S., Porta, R. N. T., Magalhães, H. L. F., Santos, A. C. Q., Viana V. H. V., Gomes, C. K., & Lima, G. B. A. (2020). Thermo-fluid dynamics analysis of fire smoke dispersion and control strategy in buildings. *Energies,* 13(22), 6000-6027.

Harrison, R., & Spearpoint, M. J. (2006). Smoke management issues in buildings with large enclosures. Paper presented at *The Engineering: Conference Contributions, Melbourne*, Australia 1-3 November.
Hurley J. M. (2016). *SFPE Handbook of Fire Protection Engineering.* Fifth Edition, New York, Springer.

Jiao, A., Lin, W., Cai, B., Wang, H., Chen, J., Zhang, M., Xiao, J., & Fan, C. (2022). Full-scale experimental study on thermal smoke movement characteristics in an indoor pedestrian street. *Case Studies in Thermal Engineering,* 34: 102029-102040.

McGrattan, K., Hostikka, S., Mcdermott, R., Floyd, J., Weinschenk, C., & Overholt, K. (2013). *Fire Dynamics Simulator (Version 6) Technical Reference Guide.* Washington: National Institute of Standards and Technology, Maryland, ABD.

Mijorski, S., & Cammelli, S. (2016). Stack effect in high-rise buildings: A review. International *Journal of High-Rise Buildings*, 5(4): 328–338.

Montes, G. C., Rojas, S. E., Kaiser, A. S., & Viedma, A. (2008). Numerical model and validation experiments of atrium enclosure fire in a new fire test facility. *Building and Environment*, 43(11): 1912–1928.

Montes, G. C., Rojas, S. E., Viedma, A & Rein, G. (2009). Experimental data and numerical modelling of 1.3 and 2.3 MW fires in a 20 m cubic atrium. *Building and Environment*, 44(9): 1827–1839.

Mowrer, F. W., Milke, J. A., & Torero, J. L. (2004). A comparison of driving forces for smoke movement in buildings. *Journal of Fire Protection Engineering*, 14(4): 237–264.

Mowrer, F. W. (2009). Driving forces for smoke movement and management. *Fire Technology*, 45(2): 147–162.

National Fire Protection Association. (2021). *NFPA 92: Standard for Smoke Control Systems*. Quincy: National Fire Protection Association.

Qin, T. X., Guo, Y. C., Chan. K. C., & Lin, W. Y. (2009). Numerical simulation of the spread of smoke in an atrium under fire scenario. *Building and Environment.* 44(1): 56-65.

Sha, H., Zhang, X., Liang, X., & Qi, D. (2022). Reduced-scale experimental and numerical investigation on the energy and smoke control performance of natural ventilation systems in a high-rise atrium. Paper presented at *The 16th Roomvent Conference* (Roomvent 2022), Xi'an China, 19 September.

Sha, H., Zhang, X., Liang, X., & Qi, D. (2023). Fire smoke control and ventilative cooling of atrium in high-rise buildings. Paper presented at *Proceedings of the 5th International Conference on Building Energy and Environment, Singapore,* 05 September.

Wang, P., Wang, X., Chen, K., &. Chen Y. (2021). Influence of opening ratios and directions of windows on natural smoke exhaust effect in atrium buildings. *Building Simulation.* 15: 571–582.

Yuen, A. C., Wang, C., Li, A., Yeoh, G. Y., Chan, N. Q., & Chan, M. C. (2019). Natural ventilated smoke control simulation case study using different settings of smoke vents and curtains in a large atrium. *Fire*, 2(1): 7-25.

Zhang, H., Wang, J., & Du, C. (2021). Experimental study on the effect of segmented smoke exhaust on smoke exhaust of ultra-thin and tall atrium. *Case Studies in Thermal Engineering,* 28: 101560.